ONLINE APPENDIX-Supplemental Data

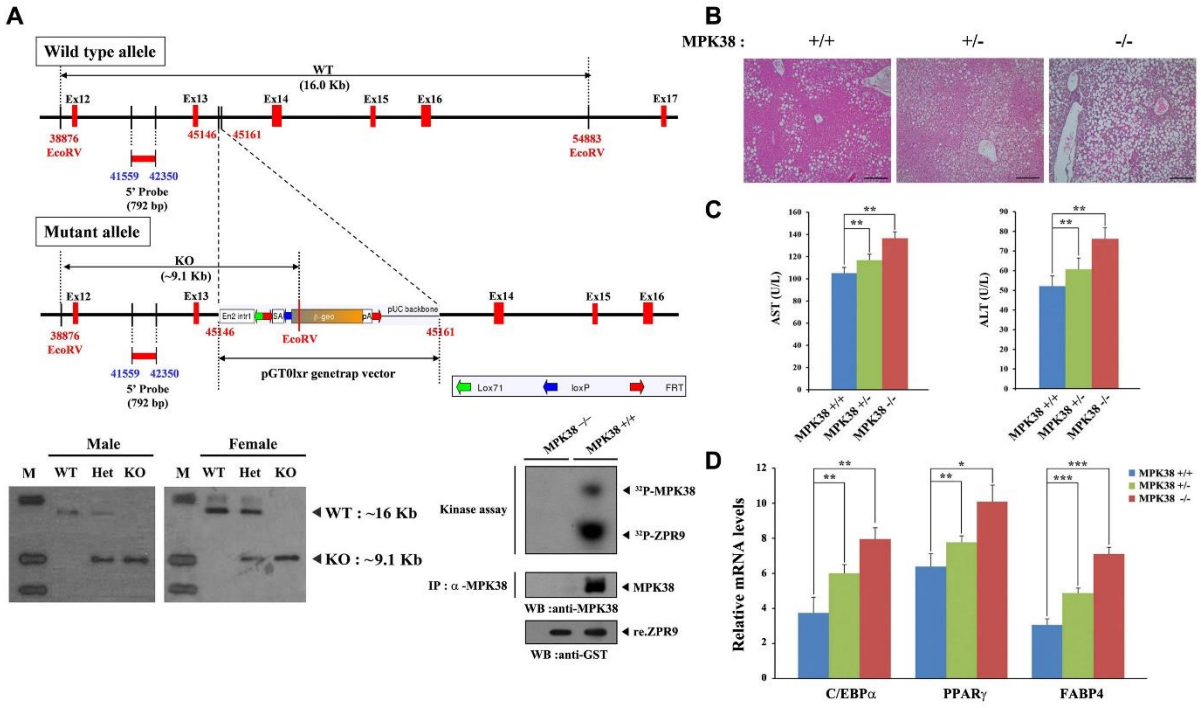

Fig. S1. MPK38-null male mice display abnormal lipid metabolism.
(**A**) Generation of MPK38$^{-/-}$ mice using a gene trap embryonic stem (ES) cell line AR081 (Mutant Mouse Regional Resource Center at UC Davis, USA). Schematic diagram of the gene trap insertion into the MPK38 gene (upper). The gene trap vector was inserted into exons (Ex) 13-14. An *EcoR*V site was introduced into the target MPK38 locus; therefore, the ~16 kb and ~9.1 kb *Eco*RV fragments indicated by the lines represent the wild-type and mutant alleles, respectively. Southern blot analysis of tail DNA from a litter of newborn pups from the MPK38 intercross (lower left). The immunoprecipitated MPK38 from MEF cells expressing MPK38 (+/+) or not (-/-) was assayed for its kinase activity using recombinant ZPR9 as a substrate (lower right). M, DNA size marker; WT, wild-type; Het, heterozygous; KO, knockout; ^{32}P, ^{32}P incorporation; IP, immunoprecipitation; WB, western blot; re., recombinant. (**B**) Representative images of paraffin-embedded sections stained with hematoxylin and eosin prepared from the livers of 7-month-old male MPK38$^{+/+}$, MPK38$^{+/-}$, and MPK38$^{-/-}$ mice fed a standard diet (n = 8-10 mice per group). Scale bar, 100 μm. (**C**) The activities of circulating aspartate aminotransferase (AST) and alanine aminotransferase (ALT). (**D**) mRNA expression of adipogenic regulators in epididymal WAT. n = 6 mice per group, *p < 0.05, **p < 0.01, ***p < 0.001 *versus* male MPK38$^{+/+}$ mice (C, D). Data were analyzed using one-way ANOVA. qPCR was performed in duplicate and repeated at least 2-3 times with similar results (D).

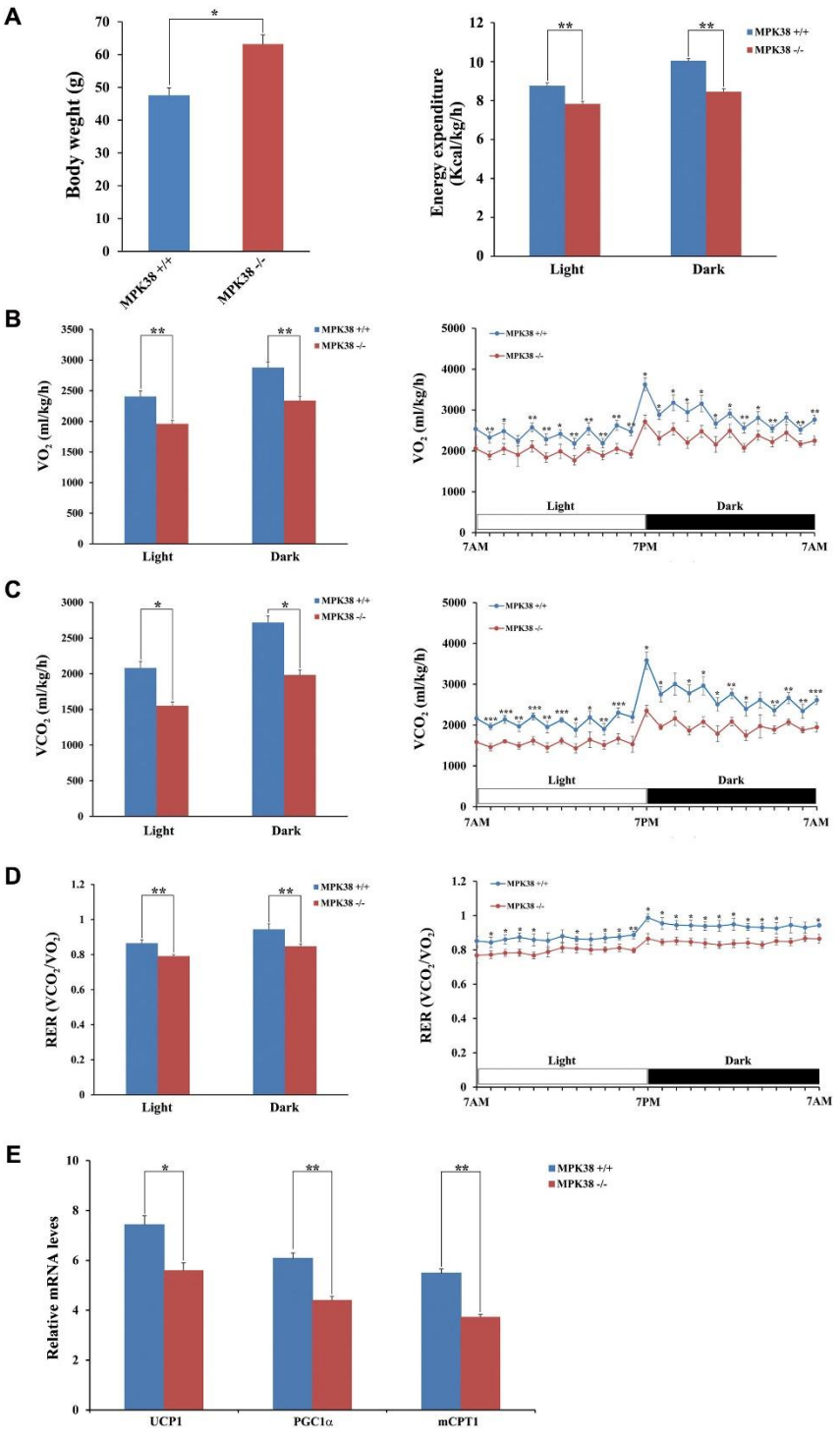

Fig. S2. MPK38-null mice expend less energy.

(**A-D**) Body mass and energy expenditure (A), oxygen consumption profiles (B), carbon dioxide generation profiles (C), and RER profiles (D) of male MPK38$^{+/+}$ and MPK38$^{-/-}$ mice during the light and dark periods (n = 6 mice per group). (**E**) mRNA expression of thermogenic regulators in BAT. n = 6 mice per group, *p < 0.05, **p <

0.01, ***$p < 0.001$ *versus* male MPK38$^{+/+}$ mice (A-E). Metabolic rates were measured by indirect calorimetry in male MPK38$^{+/+}$ and MPK38$^{-/-}$ mice fed a standard diet (7 months of age) using the OxyletPro™ System (PANLAB, Cornella, Spain). Data were analyzed using one-way (A, E) or two-way (B-D) ANOVA.

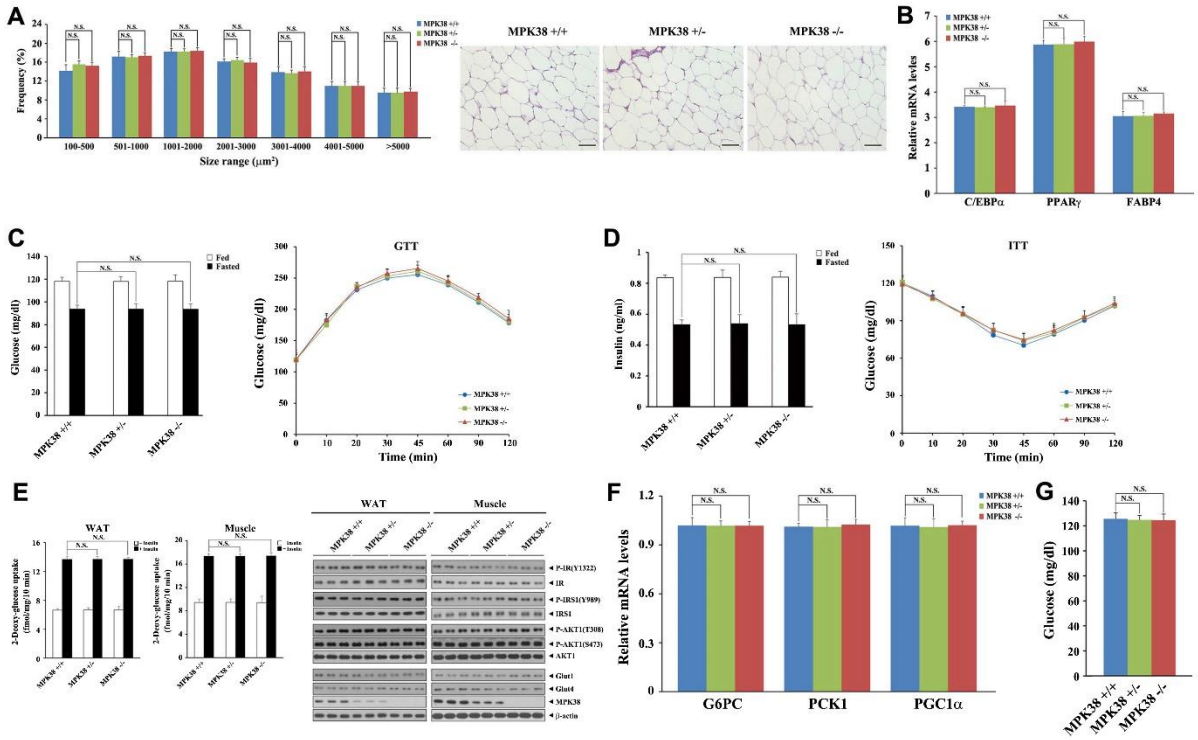

Fig. S3. MPK38 has no effect on the diet-induced metabolic disturbances in HFD-fed female mice.

(**A**) The size distribution of adipocytes (left) and representative images of paraffin-embedded epididymal WAT sections stained with hematoxylin and eosin (right) in HFD-fed MPK38$^{+/+}$, MPK38$^{+/-}$, and MPK38$^{-/-}$ female mice (n = 6-8 mice per group). Scale bar, 100 μm. (**B**) mRNA expression of adipogenic regulators in epididymal WAT. (**C, D**) Blood glucose and insulin concentrations in the fed and fasted (24 h) states, and the results of glucose and insulin tolerance tests (n = 6 mice per group). N.S. compared with controls (for GTT/ITT) or fasted controls. The statistical analyses were performed using two-way ANOVA. (**E**) *In vitro* ^{14}C-2-deoxy-glucose uptake in the presence or absence of 100 nM human insulin (left). n = 6 mice per group, N.S. compared with controls treated with insulin, determined by two-way ANOVA. IRS-PI3K signaling after *in vivo* insulin stimulation by injection into the caudal vena cava was assessed by immunoblotting (right, n = 3 mice per group). (**F, G**) mRNA expression of gluconeogenic genes in the liver (F) and the circulating concentration of glucose (G).

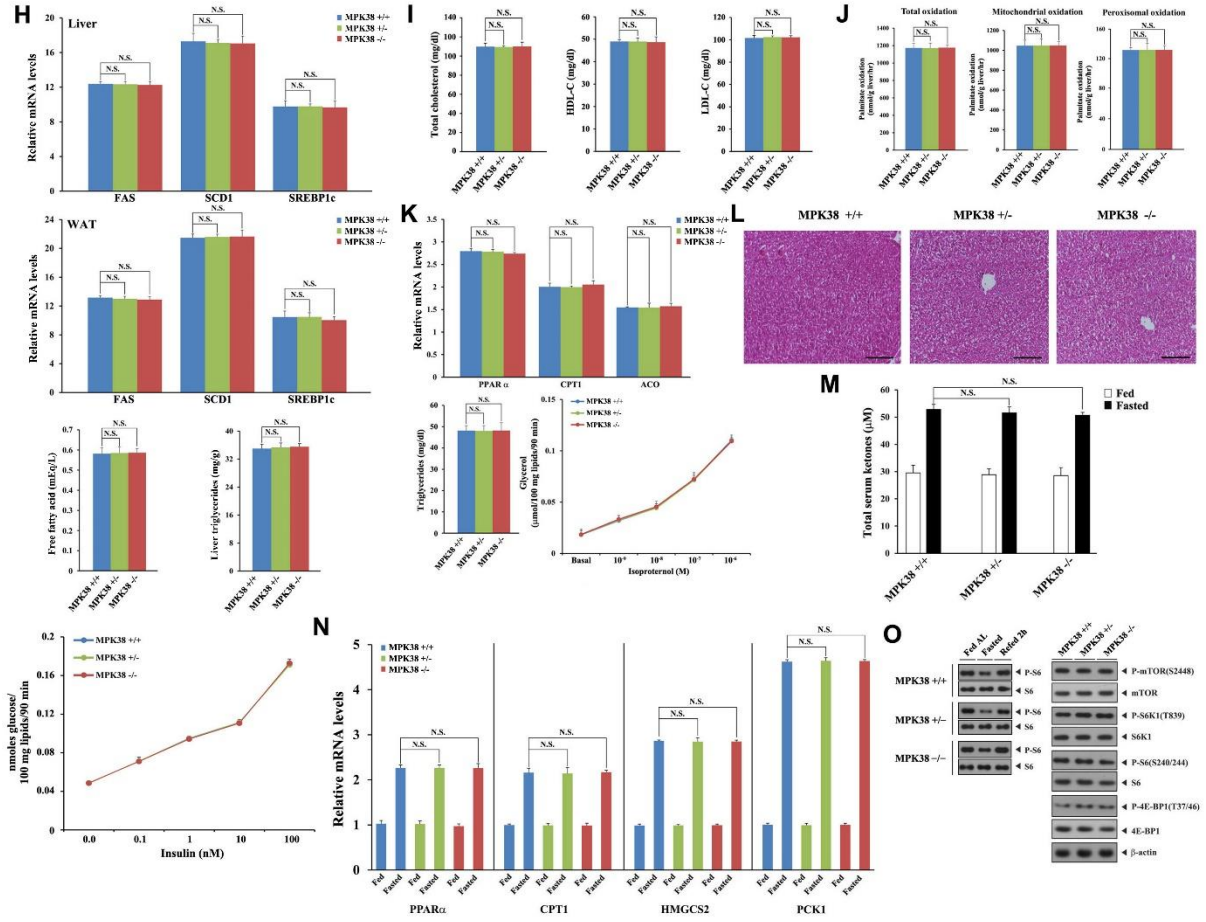

Fig. S3 (continued).

(**H**) mRNA expression of lipogenic genes in liver and epididymal WAT (top and 2nd panels), the concentrations of circulating free fatty acids and liver triglycerides (3rd panel), and the lipogenic capacity of adipocytes (bottom). (**I**) The circulating concentrations of total cholesterol, HDL-C, and LDL-C. (**J**) Measurement of hepatic β-oxidation using ^{14}C-labeled palmitate. (**K**) The mRNA expression of fatty acid oxidative genes in epididymal WAT (upper), circulating triglyceride concentration (lower left), and the isoproterenol-stimulated lipolytic response of isolated adipocytes (lower right). (**L**) Representative images of paraffin-embedded liver sections stained with hematoxylin and eosin (n = 6-8 mice per group). Scale bar, 100 μm. (**M, N**) The total ketone body concentrations in fed and fasted (24 h) blood (M) and mRNA expression of key ketogenic genes in livers (N). n = 6 mice per group, N.S. compared with fasted control. The statistical analyses were performed using two-way ANOVA. (**O**) The phosphorylation levels of S6(Ser240/244) in liver lysates from *ad libitum*-fed, fasted (24 h), and refed (2 h) female MPK38$^{+/+}$, MPK38$^{+/-}$, and MPK38$^{-/-}$ mice fed an HFD (left). mTORC1 signaling in liver lysates (right). n = 6 mice per group, N.S. compared with controls (A, B, F-K). N.S.: no significant difference. The controls were HFD-fed female MPK38$^{+/+}$ mice. Data were analyzed using one-way ANOVA, unless indicated.

qPCR was performed in duplicate and repeated at least 2-3 times with similar results (B, F, H, K, N).

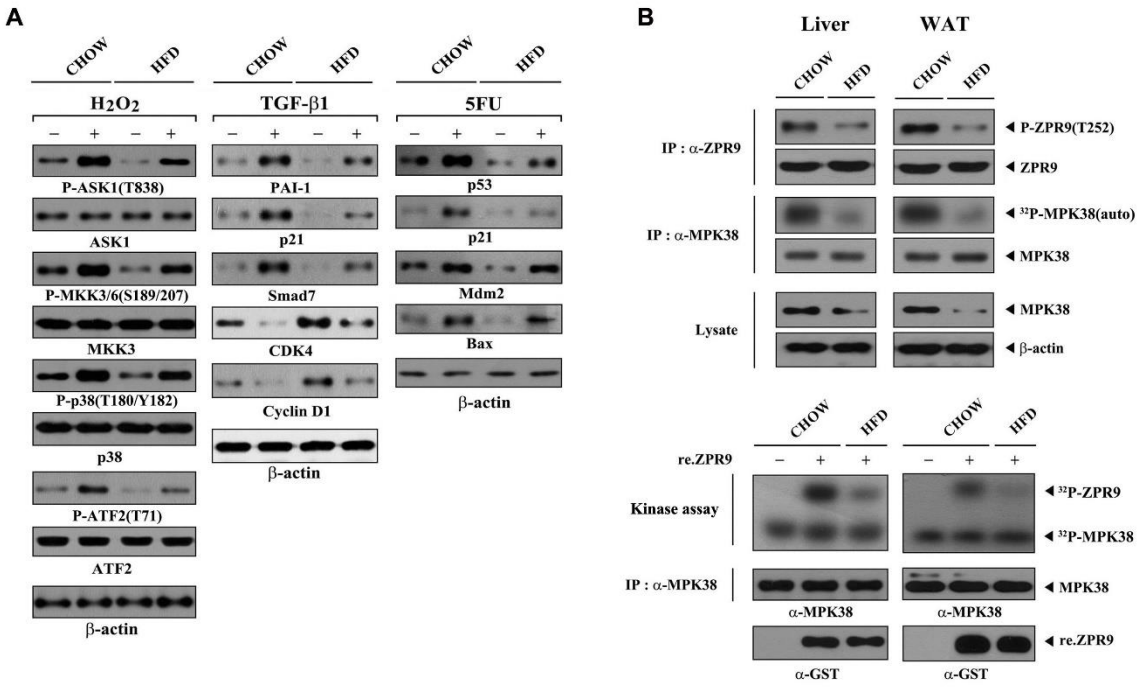

Fig. S4. Comparison of the activation of ASK1/TGF-β/p53 signaling and MPK38 kinase activity and expression in male mice fed chow or a high-fat diet.

(**A**) Isolated hepatocytes from normal chow diet (CHOW)- and high-fat diet (HFD)-fed male C57BL/6N mice that were treated with (+) or without (−) the ASK1/TGF-β/p53 stimuli H_2O_2 (2 mM, 30 min), TGF-β1 (100 pM, 20 h), or 5FU (0.38 mM, 30 h); cell lysates were immunoblotted with phospho-specific antibodies for ASK1(Thr845), MKK3/6(Ser189/207), p38(Thr180/Tyr182), and ATF2(Thr71), and antibodies for PAI-1, p21, cyclin D1, Smad7, CDK4, ASK1, p38, MKK3, ATF2, Mdm2, p53, and Bax, to determine the level of activation of ASK1/TGF-β/p53 signaling. (**B**) Comparison of the expression and activity of MPK38 in mice fed chow or a high-fat diet. Liver or WAT lysates from CHOW- and HFD-fed male C57BL/6N mice were immunoprecipitated with the indicated antibodies, followed by immunoblot analysis using a phospho-specific antibody for ZPR9 Thr252 or an *in vitro* kinase assay. ^{32}P-MPK38(auto), autophosphorylated MPK38; ^{32}P, ^{32}P incorporation; P, phosphorylated.

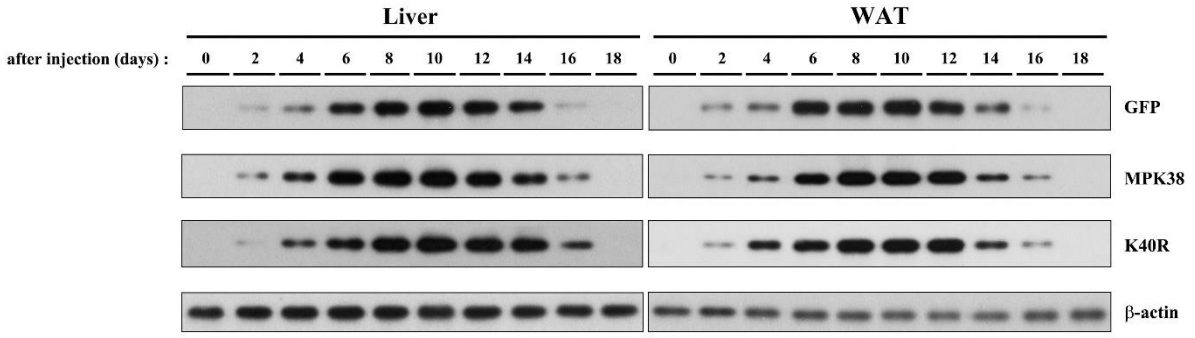

Fig. S5. Analysis of adenovirus-mediated expression of WT and kinase-dead (K40R) MPK38 in both liver and WAT.

Adenoviral expression in both liver and WAT was analyzed by immunoblotting and adenoviruses expressed WT and kinase-dead (K40R) MPK38 or GFP control for ~16 days after both tail vein and epididymal fat pad injection in 6- to 7-month-old HFD-fed C57BL/6N male mice.

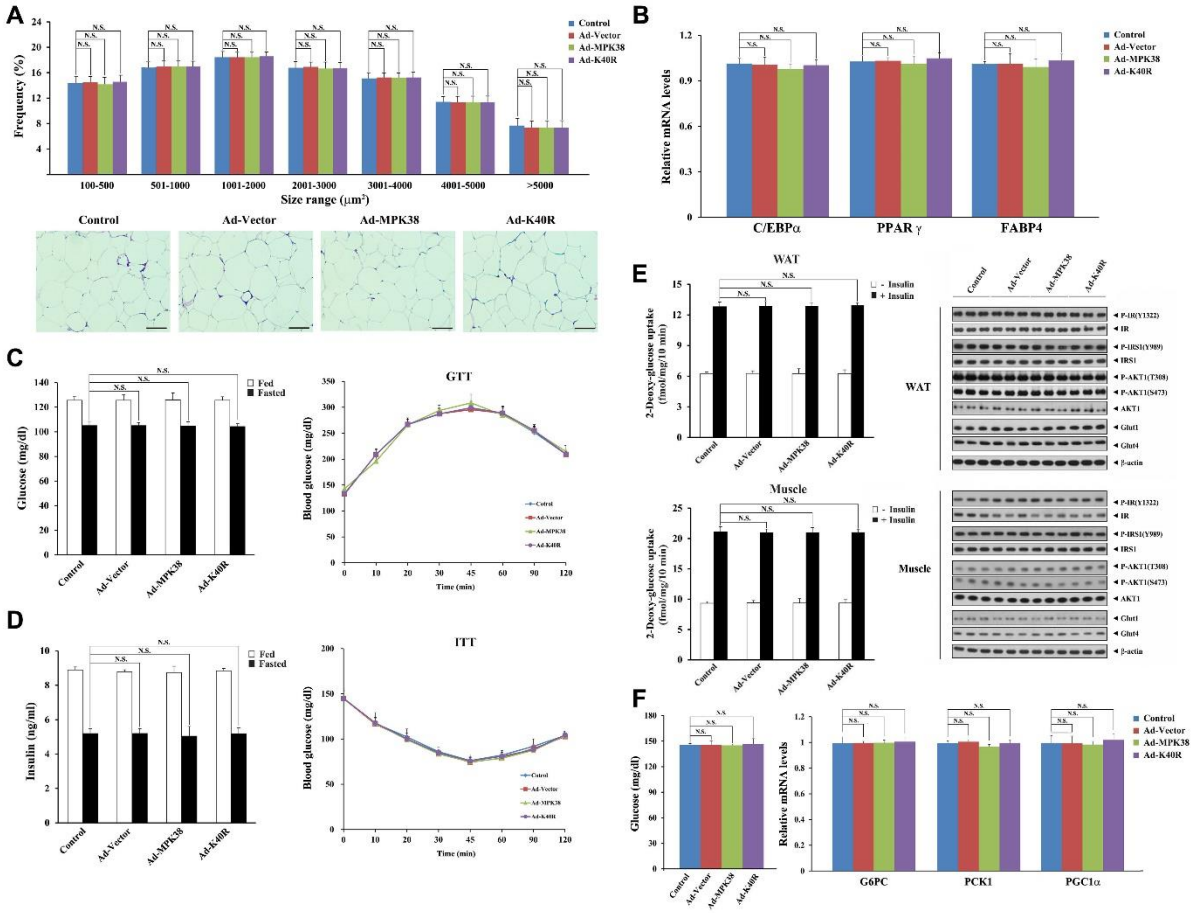

Fig. S6. Lack of an MPK38-mediated improvement in metabolism following the restoration of MPK38 expression in HFD-fed female mice.

(**A**) The size distribution of adipocytes (upper) and representative images of paraffin-embedded epididymal WAT sections stained with hematoxylin and eosin (lower) in HFD-fed female C57BL/6N mice infected with the indicated adenoviruses (n = 6 mice per group). Scale bar, 100 μm. (**B**) mRNA expression of adipogenic regulators in epididymal WAT. (**C, D**) Blood glucose and insulin concentrations in the fed and fasted (24 h) states, and the results of glucose and insulin tolerance tests. n = 6 mice per group, N.S. compared with controls (for GTT/ITT) or fasted controls. The statistical analyses were performed using two-way ANOVA. (**E**) *In vitro* ^{14}C-2-deoxy-glucose uptake into epididymal WAT and muscle (left). n = 6 mice per group, N.S. compared with controls treated with insulin, determined by two-way ANOVA. IRS-PI3K signaling after *in vivo* insulin stimulation by injection into the caudal vena cava was assessed by immunoblotting (right, n = 3 mice per group). (**F**) The circulating glucose concentration and mRNA expression of gluconeogenic genes in the liver.

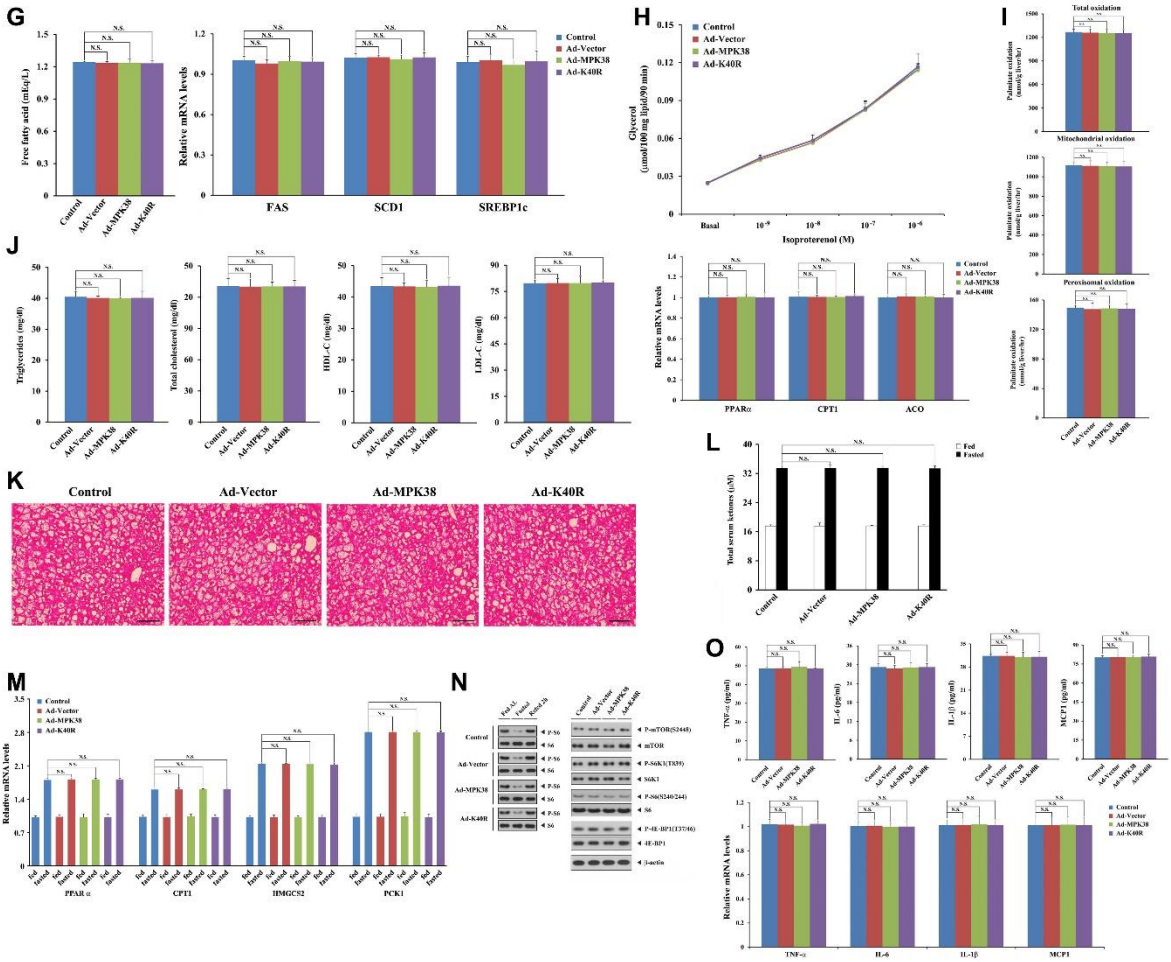

Fig. S6 (continued).

(**G**) The circulating concentration of free fatty acids and mRNA expression of lipogenic genes in epididymal WAT. (**H**) The isoproterenol-stimulated lipolytic response in isolated adipocytes (upper) and mRNA expression of fatty acid oxidative genes in epididymal WAT (lower). (**I**) Measurement of hepatic β-oxidation using ^{14}C-labeled palmitate. (**J**) The circulating concentrations of triglyceride, total cholesterol, HDL-C, and LDL-C. (**K**) Representative images of paraffin-embedded liver sections stained with hematoxylin and eosin (n = 6 mice per group). Scale bar, 100 μm. (**L, M**) The total ketone body concentrations in fed and fasted (24 h) blood (L) and mRNA expression of key ketogenic genes in livers (M). n = 6 mice per group, N.S. compared with fasted control. The statistical analyses were performed using two-way ANOVA. (**N**) Phosphorylation levels of S6(Ser240/244) in liver lysates from *ad libitum*-fed, fasted (24 h), and refed (2 h) female C57BL/6N mice infected with the indicated adenoviruses (left). mTORC1 signaling in liver lysates (right). (**O**) The circulating concentrations of proinflammatory cytokines (upper) and the relative mRNA expression of their genes in epididymal WAT (lower). n = 6 mice per group, N.S. compared with control (A, B, F-J, O). The controls were uninfected HFD-fed female C57BL/6N mice (7 months of age). N.S.: no significant difference. Data were analyzed using one-way ANOVA, unless

indicated. qPCR was performed in duplicate and repeated at least 2-3 times with similar results (B, F, G, H, M, O). Recombinant adenoviruses were administered at 1×10^9 plaque-forming units via both tail vein and epididymal fat pads of the HFD-fed female mice.

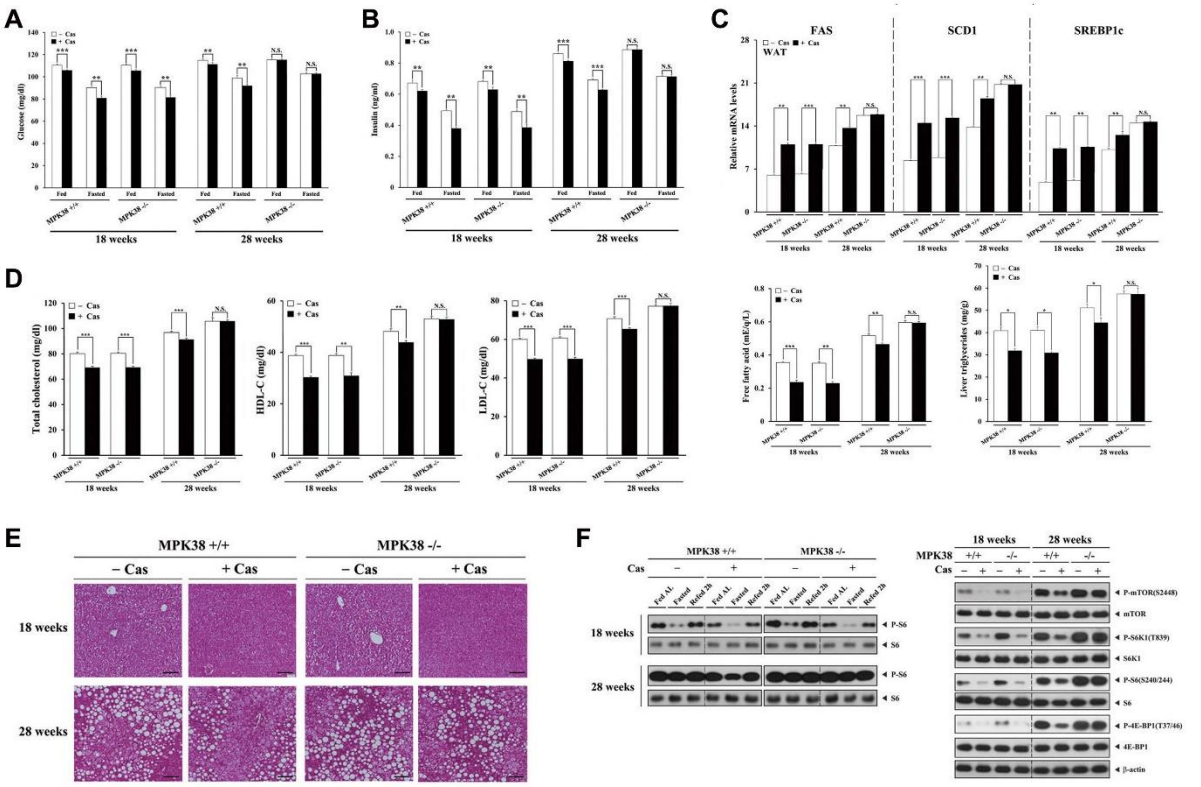

Fig. S7. Lack of castration-induced metabolic alterations in aged mature adult MPK38$^{-/-}$ male mice.

(**A, B**) blood glucose and insulin concentrations in the fed and fasted (24 h) states. n = 6 mice per group, **p < 0.01, ***p < 0.001 *versus* sham controls. The statistical analyses were performed using two-way ANOVA. (**C**) mRNA expression of lipogenic genes in epididymal WAT (upper), blood free fatty acid concentrations (lower left), and liver triglyceride content (lower right). (**D**) The circulating concentrations of total cholesterol, HDL-C, and LDL-C. (**E**) Representative images of paraffin-embedded liver sections stained with hematoxylin and eosin. n = 6 mice per group. Scale bar, 100 μm. (**F**) Phosphorylation levels of S6(Ser240/244) in liver lysates from *ad libitum*-fed, fasted (24 h), and refed (2 h) castrated mice and their sham controls (left). mTORC1 signaling in liver lysates (right). N.S.: no significant difference. n = 6 mice per group, *p < 0.05, **p < 0.01, ***p < 0.001 *versus* 4.5/7-month-old sham controls (C, D). Data were analyzed using one-way ANOVA, unless indicated. qPCR was performed in duplicate and repeated at least 2-3 times with similar results (C).

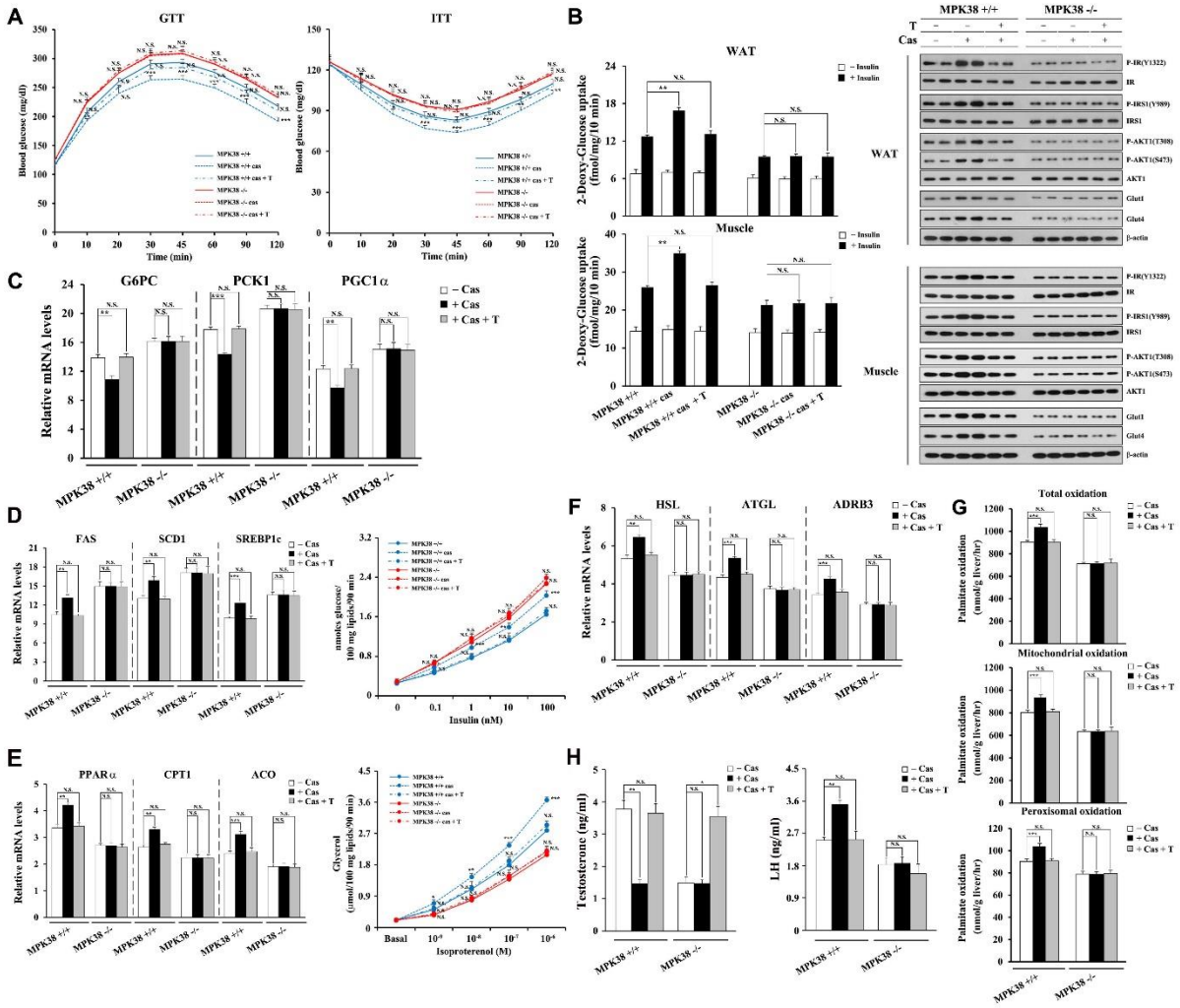

Fig. S8. Testosterone replacement has no effect on glucose and lipid metabolism in aged mature adult MPK38$^{-/-}$ male mice.

(**A**) glucose and insulin tolerance tests. n = 6 mice per group, N.S. compared with controls. The statistical analyses were performed using two-way ANOVA. (**B**) *In vitro* ^{14}C-2-deoxy-glucose uptake in the presence or absence of 100 nM human insulin (left). n = 6 mice per group, N.S. compared with controls treated with insulin, determined by two-way ANOVA. IRS-PI3K signaling after *in vivo* insulin stimulation by injection into the caudal vena cava was assessed by immunoblotting (right, n = 2 mice per group). (**C**) mRNA expression of gluconeogenic genes in the liver. (**D**) mRNA expression of lipogenic genes in epididymal WAT (left) and the lipogenic capacity of adipocytes (right). (**E**) mRNA expression of fatty acid oxidative genes in epididymal WAT (left) and the isoproterenol-stimulated lipolytic response in isolated adipocytes (right). n = 6 mice per group. N.S. compared with control mice. (**F**) mRNA expression of adipose lipolytic genes. (**G**) Measurement of hepatic β-oxidation using ^{14}C-labeled palmitate. (**H**) Serum levels of testosterone and LH, determined by ELISA kits (E-EL-M0155 & M3053; Elabscience). n = 6 mice per group, **p* < 0.05, ***p* < 0.01, ****p* <

0.001 *versus* controls. N.S.: no significant difference. The controls were uncastrated WT ($MPK38^{+/+}$) or $MPK38^{-/-}$ males (7 months of age). Data were analyzed using one-way ANOVA, unless indicated. qPCR was performed in duplicate and repeated 3 times with similar results (C-F). T indicates testosterone pellet implantation.

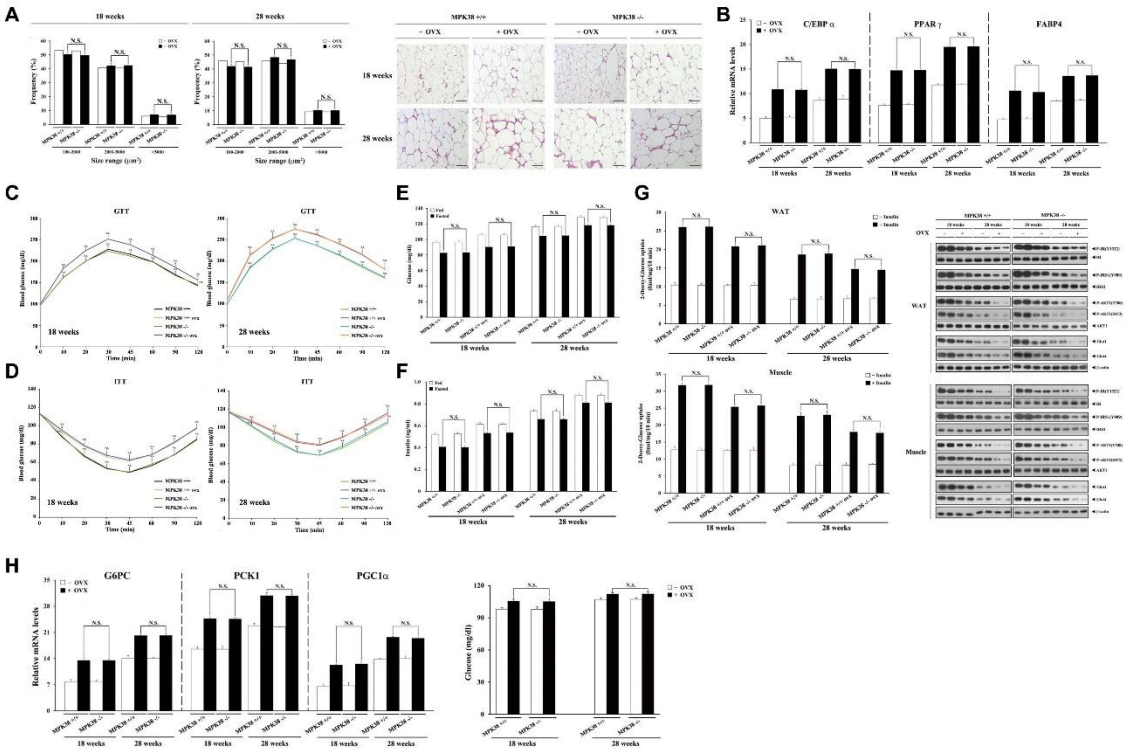

Fig. S9. MPK38 has no effect on the neutering-induced altered metabolism in mature adult female mice.

(**A**) The size distribution of adipocytes (left) and representative images of paraffin-embedded epididymal WAT sections stained with hematoxylin and eosin (right) in ovariectomized and non-ovariectomized female MPK38$^{+/+}$ or MPK38$^{-/-}$ mice (n = 6 mice per group). Scale bar, 100 μm. (**B**) mRNA expression of adipogenic regulators in epididymal WAT. (**C-F**) The results of glucose and insulin tolerance tests (C, D), and blood glucose and insulin concentrations in the fed and fasted (24 h) states (E, F). n = 6 mice per group, N.S. compared with fasted ovariectomized or non-ovariectomized MPK38$^{+/+}$ mice. The statistical analyses were performed using two-way ANOVA (E and F). (**G**) *In vitro* ^{14}C-2-deoxy-glucose uptake into epididymal WAT and muscle (left). n = 6 mice per group, N.S. compared with ovariectomized or non-ovariectomized MPK38$^{+/+}$ mice treated with insulin, determined by two-way ANOVA. IRS-PI3K signaling after *in vivo* insulin stimulation by injection into the caudal vena cava was assessed by immunoblotting (right, n = 2 mice per group). (**H**) mRNA expression of gluconeogenic genes in the liver (left) and the circulating concentration of glucose (right).

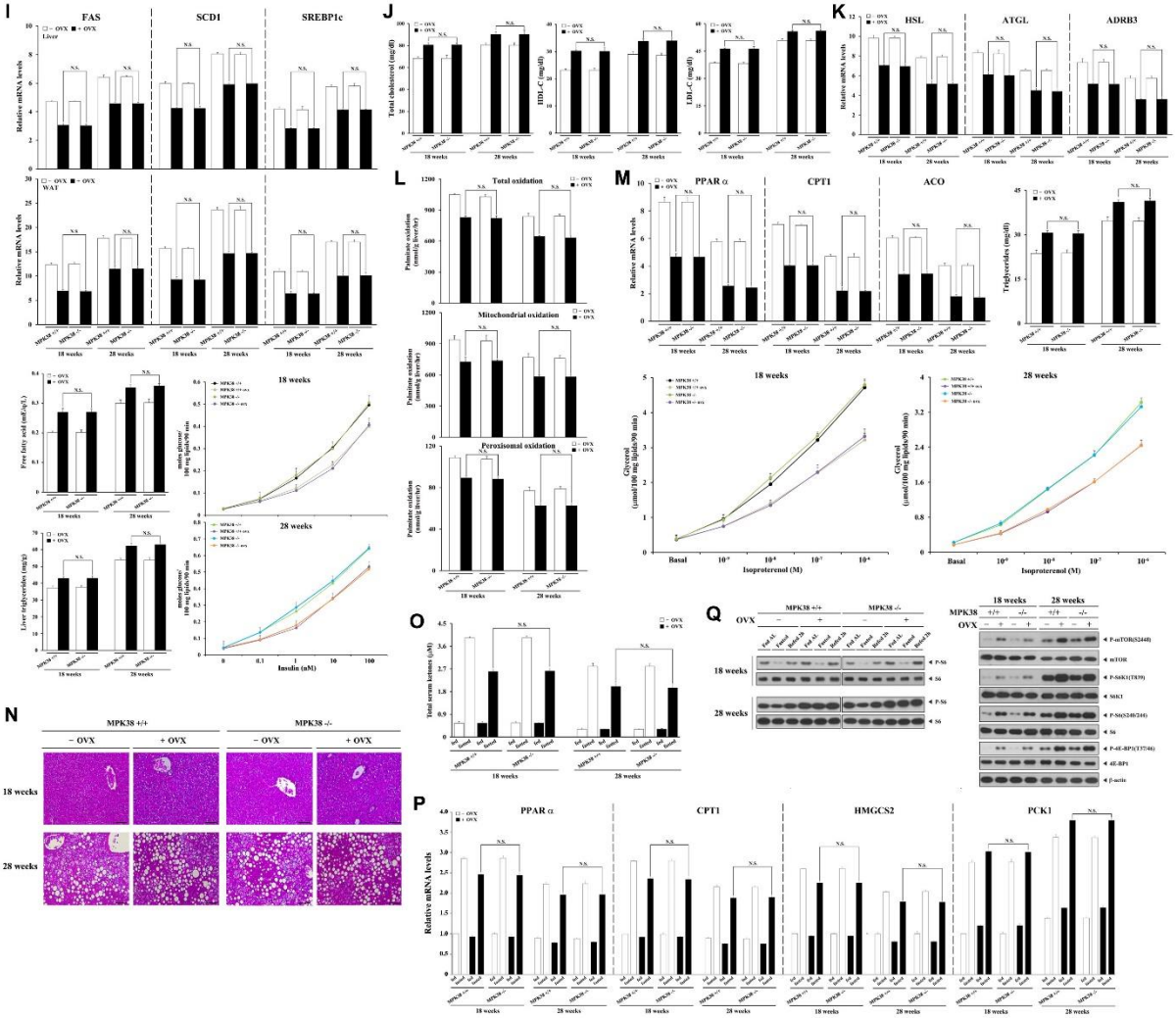

Fig. S9 (continued).

(**I**) mRNA expression of lipogenic genes in liver and epididymal WAT (top and 2nd), the circulating concentration of free fatty acids (3rd, left), liver triglyceride content (bottom, left), and the lipogenic capacity of adipocytes (3rd and bottom, right). (**J**) The circulating concentrations of total cholesterol, HDL-C, and LDL-C. (**K**) mRNA expression of adipose lipolytic genes. (**L**) Measurement of hepatic β-oxidation using ^{14}C-labeled palmitate. (**M**) mRNA expression of fatty acid oxidative genes in epididymal WAT (upper left), circulating triglyceride (upper right), and the isoproterenol-stimulated lipolytic response in isolated adipocytes (lower). n = 6 mice per group. N.S. compared with ovariectomized or non-ovariectomized MPK38$^{+/+}$ mice. (**N**) Representative images of paraffin-embedded sections stained with hematoxylin and eosin prepared from the livers of ovariectomized and non-ovariectomized MPK38$^{+/+}$ or MPK38$^{-/-}$ mice (n = 6 mice per group). Scale bar, 100 μm. (**O, P**) The total ketone body concentration in fed and fasted (24 h) blood (O) and mRNA expression of key ketogenic genes in livers (P). n = 6 mice per group, N.S. compared with fasted ovariectomized MPK38$^{+/+}$ mice. The statistical analyses were performed using two-way ANOVA. (**Q**) Phosphorylation levels of S6(Ser240/244) in liver lysates

from *ad libitum*-fed, fasted (24 h), and refed (2 h) ovariectomized and non-ovariectomized MPK38$^{+/+}$ or MPK38$^{-/-}$ mice (left). mTORC1 signaling in liver lysates (right). n = 6 mice per group, N.S. compared with ovariectomized MPK38$^{+/+}$ mice (4.5/7 months of age) (B, H, I-L). N.S.: no significant difference. Data were analyzed using one-way ANOVA, unless indicated. qPCR was performed in duplicate and repeated at least 2-3 times with similar results (B, H, I, K, M, P).

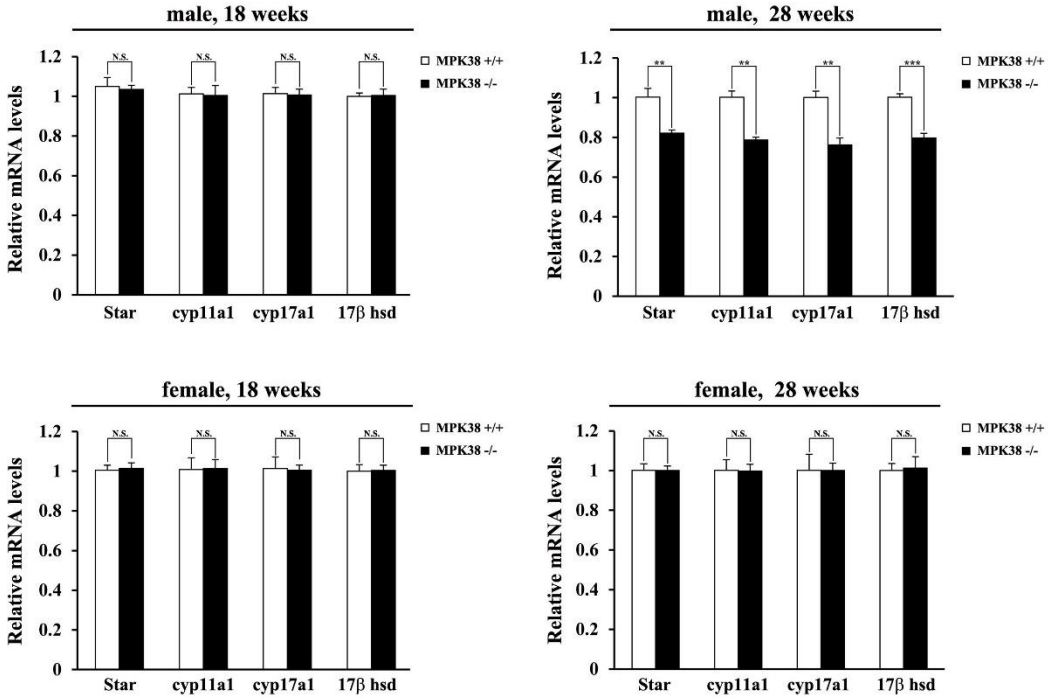

Fig. S10. MPK38 deficiency causes a decrease in steroidogenesis in aged mature adult male mice.

mRNA expression of steroidogenic genes involved in steroid hormone synthesis in the testes (upper panels) and ovaries (lower panels) of MPK38$^{+/+}$ and MPK38$^{-/-}$ mice fed a standard diet (4.5/7 months of age). n = 8 mice per group, $^{**}p < 0.01$, $^{***}p < 0.001$ *versus* MPK38$^{+/+}$ controls. N.S.: no significant difference. qPCR was performed in duplicate and repeated 3 times with similar results.

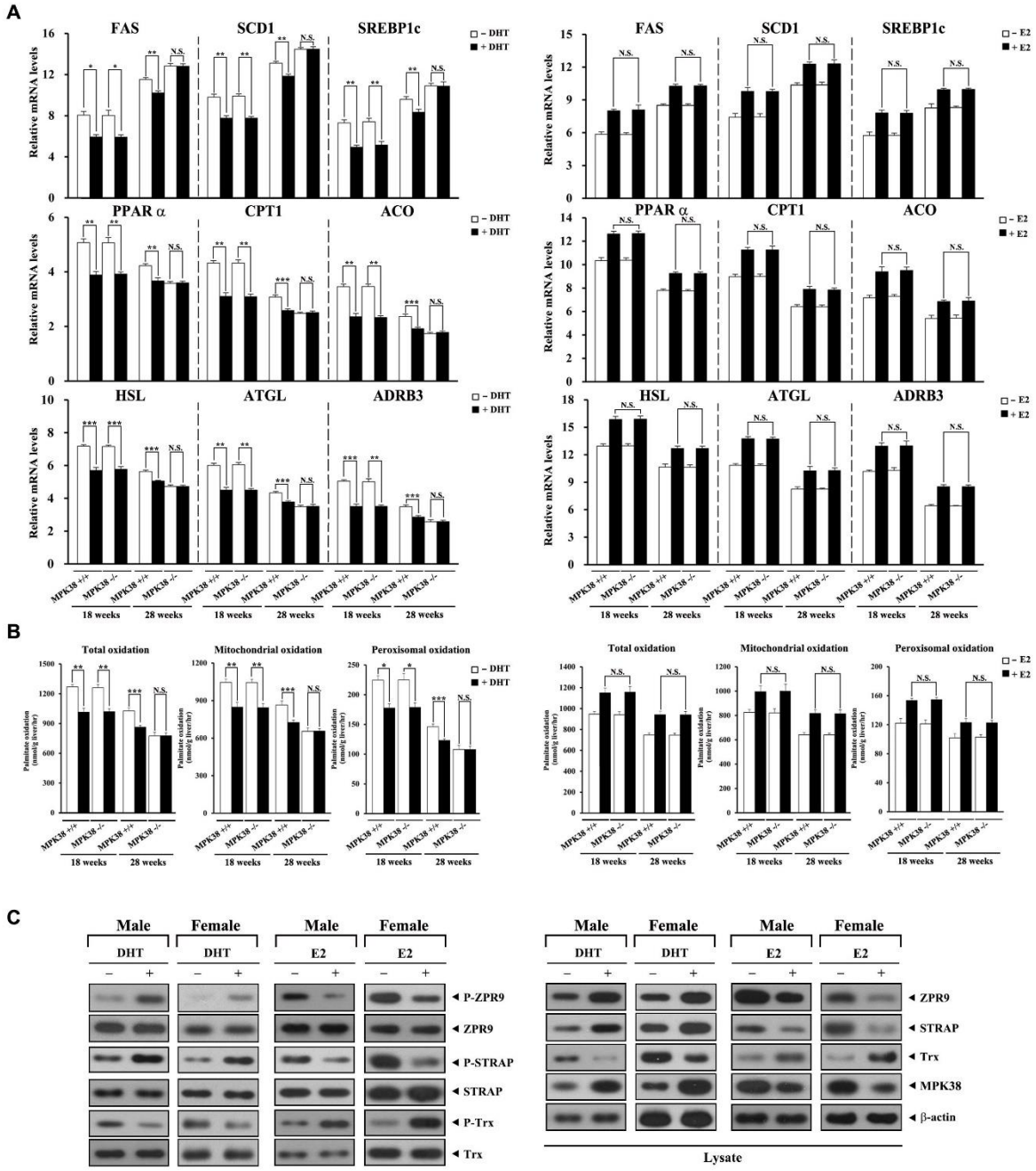

Fig. S11. Analysis of the effects of testosterone and estrogen on liver lipid metabolism and MPK38 kinase activity using hepatocytes from mature adult mice.

(**A**) mRNA expression of lipogenic genes (FAS, SCD1, and SREBP1c), fatty acid oxidative genes (PPARα, CPT1, and ACO), and lipolytic genes (HSL, ATGL, and ADRB3) in hepatocytes treated with (+) or without (−) DHT or E2 (10 nM each) for 24 h. Hepatocytes were obtained from male (left panels) or female (right panels) C57BL/6N mice (4.5/7 months of age). (**B**) Hepatic β-oxidation was measured by

incubation of liver extracts treated with or without DHT or E2 with ^{14}C-labeled palmitate. (**C**) MPK38 kinase activity in hepatocytes, which were obtained from 4.5-month-old mice, treated with DHT or E2 was determined by immunoblotting with the indicated antibodies. n = 8 mice per group, *$p < 0.05$, **$p < 0.01$, ***$p < 0.001$ *versus* controls. N.S.: no significant difference. The controls were untreated MPK38$^{+/+}$ (or MPK38$^{-/-}$) mice (A and B, left panels) or treated MPK38$^{+/+}$ mice (A and B, right panels). Data were analyzed using one-way ANOVA. P, phosphorylated.

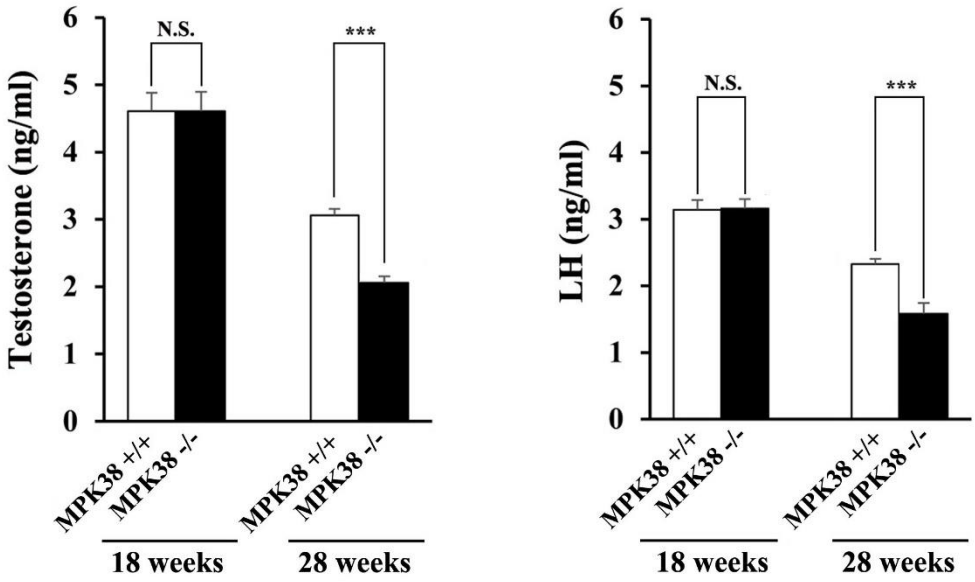

Fig. S12. MPK38 deficiency causes a decrease in testosterone and luteinizing hormone (LH) production in aged mature adult male mice.

The circulating concentrations of testosterone (left) and LH (right) in MPK38$^{+/+}$ and MPK38$^{-/-}$ male mice (4.5/7 months of age) fed a standard diet were quantified using ELISAs. n = 8 mice per group, ***p < 0.001 *versus* MPK38$^{+/+}$ controls. N.S.: no significant difference.

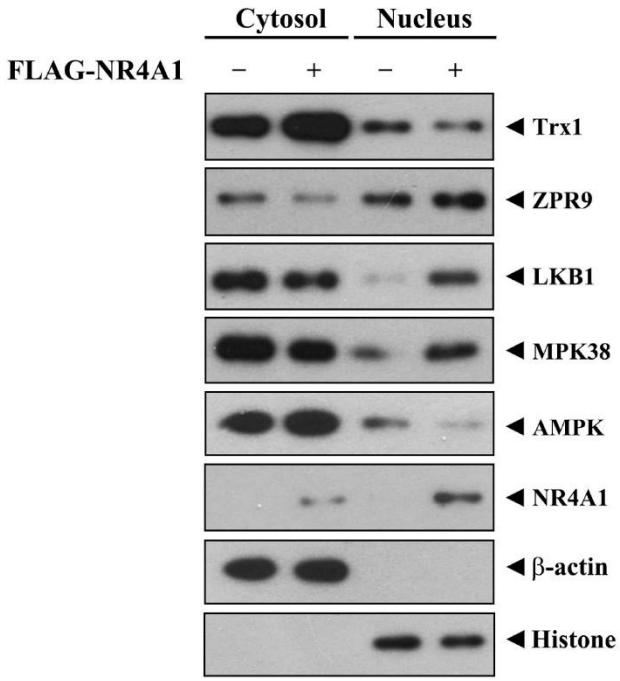

Fig. S13. Greater nuclear localization of MPK38 and its positive regulator ZPR9 in Nr4a1-overexpressing cells.

Cytoplasmic (cytosol) and nuclear (nucleus) fractions of HepG2 cells that had been transfected with (+) or without (−) FLAG-tagged Nr4a1 were obtained and used for immunoblot analyses using antibodies for Trx1, ZPR9, LKB1, MPK38, AMPK, FLAG(M2), β-actin, and histone to determine the effect of Nr4a1 on the subcellular localization of these proteins.

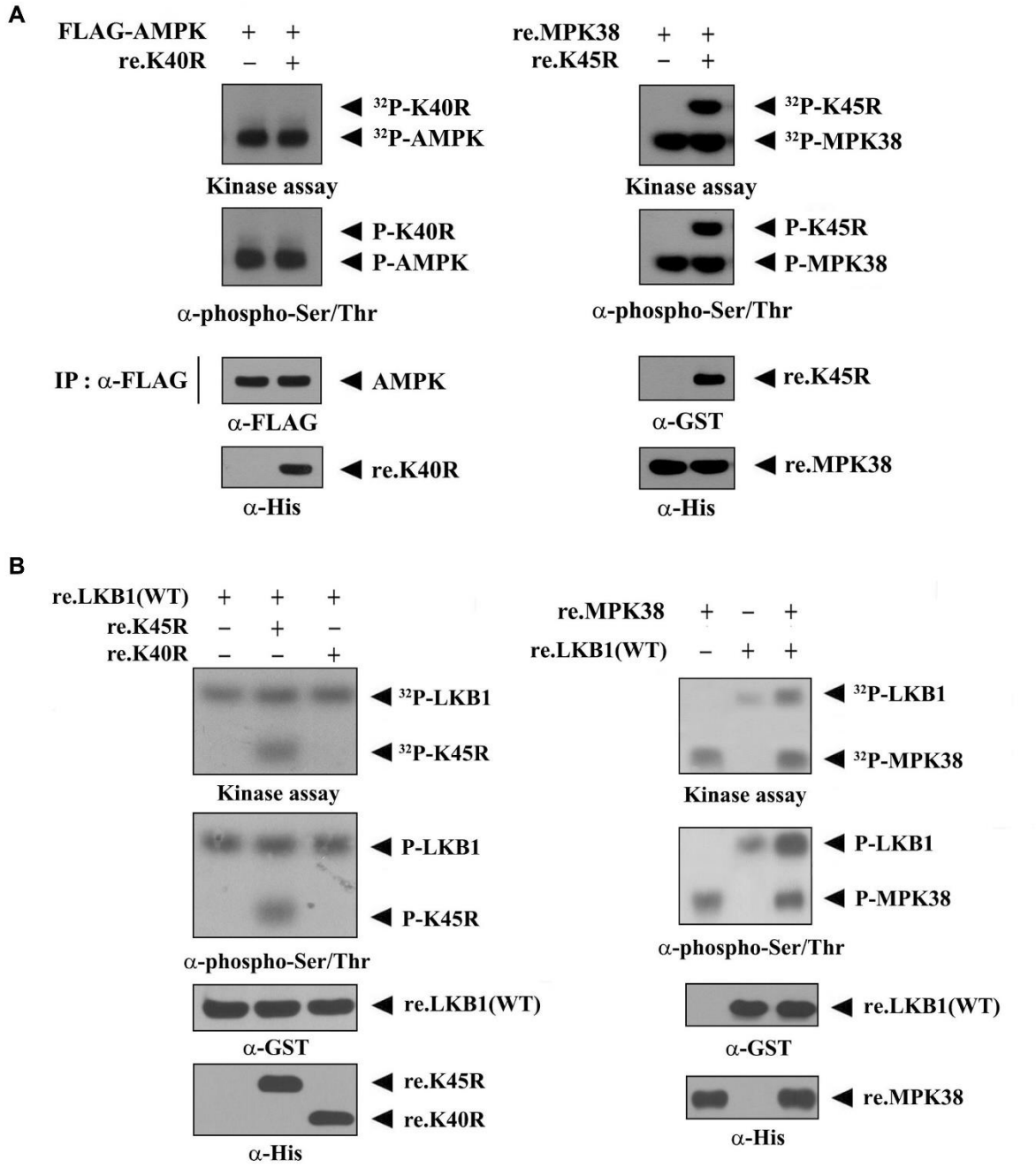

Fig. S14. MPK38 functions as a potential upstream kinase of LKB1 and AMPK. (**A**) For *in vitro* AMPK/MPK38 kinase assays, approximately 3 μg of recombinant kinase-dead MPK38 (K40R) or AMPK (K45R) were mixed with 5 μCi of [γ-^{32}P]-ATP in 20 μl of each kinase buffer (see Supplementary Materials) and incubated with immunoprecipitated AMPK (~2 μg) for 20 min at 30 ºC (left) or recombinant MPK38 (~2 μg) for 15 min at 37 °C (right), with frequent gentle mixing. The phosphorylation levels were also confirmed by immunoblot analysis using an anti-phospho-Ser/Thr antibody (2nd panels). (**B**) For *in vitro* LKB1/MPK38 kinase assays, approximately 3

μg of recombinant kinase-dead MPK38 (K40R) and AMPK (K45R) (left) or wild-type LKB1 (right) were mixed with 5 μCi of [γ-^{32}P]-ATP in 20 μl of each kinase buffer (see Supplementary Materials) and incubated with recombinant LKB1 (~2 μg) at 30 ºC for 30 min (left) or MPK38 (~2 μg) for 15 min at 37 °C (right), with gentle mixing. The phosphorylation levels were also determined by immunoblotting using an anti-phospho-Ser/Thr antibody (2nd panels). re., recombinant; ^{32}P, ^{32}P incorporation; P, phosphorylated.

Table S1. Primer sequences used in this study.

Real-Time PCR primers for target genes

Gene	Sequence	
18S rRNA (mouse)	sense	5'-GTAACCCGTTGAACCCCATT-3'
	antisense	5'-CCATCCAATCGGTAGTAGCG-3'
ACO (mouse)	sense	5'-GCCAATGCTGGTATCGAAGAA-3'
	antisense	3'-GGAATCCCACTGCTGTGAGAA-3'
ADRB3 (mouse)	sense	5'-TGAAACAGCAGACAGGGACA-3'
	antisense	5'-GGATGTCCATACCAGGGCAC-3'
ATGL (mouse)	sense	5'-CTGAGAATCACCATTCCCACATC-3'
	antisense	5'-CACAGCATGTAAGGGGGAGA-3'
CPT1 (mouse)	sense	5'-ACCACTGGCCGAATGTCAAG-3'
	antisense	5'-AGCGAGTAGCGCATGGTCAT-3'
FAS (mouse)	sense	5-TGCTCCAGGGATAACAGC-3'
	antisense	5'-CCAAATCCAACATGGGACA-3'
G6PC (mouse)	sense	5'-TGGTAGCCCTGTCTTTCTTTG-3'
	antisense	5'-TTCCAGCATTCACACTTTCCT-3'
HSL (mouse)	sense	5'-TTCTCCAAAGCACCTAGCCAA-3'
	antisense	5'-TGTGGAAAACTAAGGGCTTGTTG-3'
PCK1 (mouse)	sense	5'-ATCACCGCATAGTCTCTGAA-3'
	antisense	5'-ACACACACACATGCTCACAC-3'
PGC1α (mouse)	sense	5'-AGCACTCAGAACCATGCAGCAAAC-3'
	antisense	5'-TTTGGTGTGAGGAGGGTCATCGTT-3'
PPARα (mouse)	sense	5'-CTGCAGAGCAACCATCCAGAT-3'
	antisense	5'-GCCGAAGGTCCACCATTTT-3'
SCD1 (mouse)	sense	5'-ACCTGCCTCTTCGGGATTTT-3'
	antisense	5'-GTCGGCGTGTGTTTCTGAGA-3'
SREBP1 (mouse)	sense	5'- AGCTGCGTGGTTTCCAACA-3'
	antisense	5'-CCTCATGTAGGAATACCCTCCTCAT-3'
TNF-α (mouse)	sense	5'-ACGGCATGGATCTCAAAGAC-3'
	antisense	5'-AGATAGCAAATCGGCTGACG-3'
IL-6 (mouse)	sense	5'-GTCCTTCCTACCCCAATTTCCA-3'
	antisense	5'-TAACGCACTAGGTTTGCCGA-3'
IL-1β (mouse)	sense	5'-TGTGAAATGCCACCTTTTGA-3'
	antisense	5'-GGTCAAAGGTTTGGAAGCAG-3'
MCP1 (mouse)	sense	5'-CCACTCACCTGCTGCTACTCA-3'
	antisense	5'-TGGTGATCCTCTTGTAGCTCTCC-3'
Cyp11a1 (mouse)	sense	5'-CCTATTCCGCTTTTCCTTTGAGTCC-3'
	antisense	5'-CGCTCCCCAAATATAACACTGCTG-3'
Cyp17a1 (mouse)	sense	5'-TCGGCCCCAGATGGTGACTC-3'
	antisense	5'-TGGTCCGACAAGAGGCCTAGAG-3'
17β-hsd (mouse)	sense	5'-AGTGTGGGAGGCTTGATGGGA-3'
	antisense	5'-CACTTCGTGGAATGGCAGTCC-3'

PCR primers for recombinant adenoviruses

Gene	Sequence	
MPK38	sense	5'-GTAACTATAACGGTCATGAAAGATTATGACGAACTCCTCAAA-3'
	antisense	5'-ATTACCTCTTTCTCCTCACATCTTGCAGCCAGACAAGAT-3'

Antibodies and oligonucleotides. Anti-phospho-S6(S240/244) (#5364), anti-phospho-mTOR(S2448) (#5536), anti-phospho-ASK1 (T845) (#3765), anti-phospho-MKK3/6(S189/207) (#9231), anti-phospho-p38 (T180/Y182) (#4511), anti-phospho-ATF2(T71) (#24329), anti-phospho-S6K1(T389) (#9206), anti-phospho-4E-BP1(T37/46) (#2855), anti-phospho-AKT1(T308) (#2965), anti-phospho-AKT1(S473) (#9018), anti-phospho-AMPKα(Thr172) (#2531), anti-phospho-ACC1(Ser79) (#11818), anti-mTOR (#2972), anti-S6K1 (#9202), anti-4E-BP1 (#9644), anti-AKT1 (#2938), anti-AMPKα (#5832), and anti-ACC1 (#4190) antibodies were purchased from Cell Signaling Technology (Danvers, MA). Anti-phospho-IRβ(Y1322) (#04-300) and anti-IRβ (MABN390) antibodies were from Millipore Corp. (Bedford, MA). Anti-phospho-IRS1(Y989) (sc-17200), anti-IRS1 (sc-8038), anti-p53(DO-1) (sc-126), anti-p21 (sc-6246), anti-Mdm2 (sc-965), anti-PAI-1 (sc-5297), anti-ASK1 (sc-390275), anti-S6 (sc-74459), anti-MKK3 (sc-271779), anti-ATF2 (sc-242), anti-p38 (sc-7972), anti-Bax (sc-7480), anti-Trx (sc-271281), anti-CDK4 (sc-23896), and anti-Cyclin D1 (sc-8396) antibodies were from Santa Cruz Biotechnology (Santa Cruz, CA). Anti-phospho-Ser/Thr (ab17464), anti-GLUT1 (ab652), and anti-GLUT4 (ab654) antibodies were from Abcam (Cambridge, UK). Anti-Smad7 antibody (MAB2029) was from R&D Systems (Minneapolis, MN). Anti-β-actin antibody (A2228) was from Sigma (St. Louis, MO). F4/80-PE (1:100, #123110), Cd206-Alexa Fluor 647 (1:100, #141708), and Cd11c-FITC (1:100, #117306) were obtained from BioLegend (San Diego, CA). Anti-MPK38 and anti-ZPR9 antibodies were raised in a rabbit against recombinant full-length MPK38 and ZPR9 proteins, respectively (Young In Frontier, Seoul, Korea).

Quantitative real-time PCR (qPCR). Total RNA was extracted from cells and tissues using a TRIzol RNA isolation system (12183555; Invitrogen) according to the manufacturer's instructions and used to synthesize single-strand cDNA. The cDNA synthesis was performed using a Superscript cDNA kit (11917010; Invitrogen). qPCR was run on a LightCycler instrument using a LightCycler reaction kit (2239264; Roche Diagnostics). 20 ul qPCR reaction contained 2 μl cDNA, 200 nM primers, Taq DNA polymerase, 2.3 mM $MgCl_2$, and 2 μl SYBR green. The qPCR started at 95 °C for 15 min for pre-denaturation followed by 40 cycles (95 °C for 10s, 55 °C for 20s, and 72

°C for 30s). All samples were run in duplicate using 18S ribosomal RNA for normalizing mRNA expression.

Castration and ovariectomy. For the surgeries, mice were anesthetized with a mixture of ketamine (34 mg/kg), xylazine(6.8 mg/kg), and acepromazine (1.1 mg/kg) in saline. After the surgical site was shaved, cleaned, and disinfected with 70% alcohol. For castration, after midline abdominal incision, the testes and attached fat pads were left intact. The testes were removed through an incision, but the testicular ducts and blood vessels supplying the testes were ligated with sterile silk suture and the testicular fat pads were put back, followed by closure with sterile silk suture. For the sham castration, the testes with attached fat pads were exposed and put back without organ extirpation after abdominal incision, and the incision was closed with sterile silk suture. For ovariectomy, after midline abdominal incision, the uterus, oviducts, and ovaries with the fat pads were left intact. The ovaries were removed through an incision, but the oviduct and blood vessels supplying the ovaries were ligated with sterile silk suture and the ovarian fat pads were put back, followed by closure with sterile silk suture. For the sham ovariectomy, the oviducts, uterus, and ovaries with the fat pads were exposed and put back without organ extirpation after abdominal incision. After surgery, mice were monitored until they are fully recovered from anesthesia. Mice were used for the experiments 5-6 weeks after the surgery.

Animals. Male or female C57BL/6N (14-15 weeks of age), which were purchased from Central Lab. Animal Inc. (Seoul, Korea), were given a HFD (Research Diets, Inc. D12492, 60% kcal fat) for ~12 weeks and used for adenoviral-mediated restoration experiments. They were housed in the pathogen-free cages with unlimited access to water and food under 12 h light and 12 h darkness. All animal experiments were conducted under guidelines and regulations established by the Ethics Review Committee of Chungbuk National University (CBNUA-966-16-02) and approved by the Institutional Animal Care and Use Committee of the veterinary school at Chungbuk National University (Cheongju, Korea). Age- and sex-matched mice of the same strain were used in each experiment. Animal numbers for each experiment were determined based on reported similar experiments or our pilot experiments.